

Reconciling charmonium production and polarization data in the midrapidity region at hadron colliders within the nonrelativistic QCD framework^{*}

Zhan Sun(孙焜)¹ Hong-Fei Zhang(张鸿飞)^{2;1)}¹ School of Science, Guizhou Minzu University, Guiyang 500025, China² Department of Physics, School of Biomedical Engineering, Third Military Medical University, Chongqing 400038, China

Abstract: A thorough study reveals that the only key parameter for ψ (J/ψ , ψ') polarization at hadron colliders is the ratio $\langle O^\psi(^3S_1^{[8]}) \rangle / \langle O^\psi(^3P_0^{[8]}) \rangle$, if the velocity scaling rule holds. A slight variation of this parameter results in substantial change of the ψ polarization. We find that with equally good description of the yield data, this parameter can vary significantly. Fitting the yield data is therefore incapable of determining this parameter, and consequently, of determining the ψ polarization. We provide a universal approach to fixing the long-distance matrix elements (LDMEs) for J/ψ and ψ' production. Further, with the existing data, we implement this approach, obtain a favorable set of the LDMEs, and manage to reconcile the charmonia production and polarization experiments, except for two sets of CDF data on J/ψ polarization.

Keywords: J/ψ polarization, nonrelativistic QCD, long-distance matrix elements

PACS: 12.38.Bx, 12.39.St, 13.85.Ni **DOI:** 10.1088/1674-1137/42/4/043104

1 Introduction

Nonrelativistic QCD (NRQCD) [1] is one of the most successful effective theories describing quarkonium production and decays (for a review, see e.g. Ref. [2]). Despite its contributions, however, it is facing various challenges. Three groups [3–5] have succeeded in QCD next-to-leading order (NLO) calculations of J/ψ production and polarization at hadron colliders. However, with different fitting strategies, they have obtained quite different values of the long-distance matrix elements (LDMEs), consequently leading to different perspectives on the polarization puzzle. Recently, the LHCb Collaboration released their results for the η_c hadroproduction measurement [6]. Three groups [7–9] looked into the experimental data from different points of view. Reference [4] interpreted the almost unpolarized experimental results of the J/ψ hadroproduction measurements as the indication of $^1S_0^{[8]}$ dominance, which violates heavy quark spin symmetry (HQSS) regarding the data in Reference [6]. Others [5, 10–14], even with different philosophies, also came to similar conclusions. References [8, 9] remedied the discrepancy between the measurements of J/ψ and η_c hadroproduction. Notably, their LDMEs are

consistent with the velocity scaling rule (VSR), which is essential to the NRQCD expansion. Even so, both of them failed to explain the J/ψ polarization data in the midrapidity regions. The polarization parameter λ (in this paper, we only discuss the polarization in the helicity frame) converges in the ranges $0.05 < \lambda < 0.2$ (for $|y| < 0.6$, denoted as E1) and $0 < \lambda < 0.1$ (for $0.6 < |y| < 1.2$, denoted as E2) for the CMS experiment [15], and $-0.2 < \lambda < 0$ for the CDF experiment [16] (denoted as E3). Here λ is defined by

$$\lambda = \frac{d\sigma_T - 2d\sigma_L}{d\sigma_T + 2d\sigma_L}, \quad (1)$$

where σ_T and σ_L are the transverse and longitudinal cross sections, respectively. However, the theoretical predictions [8, 9] of λ for E1, E2 and E3 reach 0.4, 0.4 and 0.2, respectively. Taking E2 as an example, the experimental and theoretical values of the ratio of the transverse cross section to twice the longitudinal one are about 1.2 and 2.3, respectively. A successful effective theory cannot tolerate so large a discrepancy. Accordingly, Refs. [7, 8] both agree that, despite the η_c and J/ψ yield data being reconciled, the corresponding LDMEs still cannot solve the J/ψ polarization puzzle. In sum,

Received 28 November 2017, Published online 2 March 2018

^{*} Supported by National Natural Science Foundation of China (11405268, 11647113, 11705034)

1) E-mail: hfzhang@ihep.ac.cn (corresponding author)



Content from this work may be used under the terms of the Creative Commons Attribution 3.0 licence. Any further distribution of this work must maintain attribution to the author(s) and the title of the work, journal citation and DOI. Article funded by SCOAP³ and published under licence by Chinese Physical Society and the Institute of High Energy Physics of the Chinese Academy of Sciences and the Institute of Modern Physics of the Chinese Academy of Sciences and IOP Publishing Ltd

the J/ψ polarization is still among the most challenging puzzle in high energy physics waiting for new explorations.

The mess of the situation can actually be attributed to the difficulty in determining the LDMEs. As is going to be seen later in this paper, ordinary fitting procedures are incapable of tackling this problem. A practical strategy which is able to definitely either solve the J/ψ polarization puzzle or phenomenologically disprove NRQCD is urgently needed.

The recent measurement of η_c hadroproduction [6], along with the corresponding theoretical study [9], suggests that the $^1S_0^{[8]}$ channel cannot saturate the J/ψ hadroproduction, as long as the VSR and HQSS holds. Accordingly, the $^3S_1^{[8]}$ and $^3P_J^{[8]}$ channels will contribute a significant part to (in fact, dominate) the J/ψ hadroproduction. Note that the $^3P_J^{[8]}$ short-distance coefficient (SDC) and the $^3S_1^{[8]}$ LDME are both dependent on the NRQCD scale (μ_Λ), and the combination of the two channels is divergence free and μ_Λ independent¹⁾. We can consider these two channels as a unity and work out the fraction that each ingredient accounts for at a specific value of μ_Λ . In the context of the ψ hadroproduction in the midrapidity region, μ_Λ independence is approximately guaranteed [17]. To this end, its value is fixed as $\mu_\Lambda = m_c$ in our study, which is consistent with most of the existing values in the literature.

We find some interesting features in the J/ψ (and ψ') hadroproduction and polarization problem. These features can be summarized as follows and will be further demonstrated in the rest of this paper.

1) As long as the VSR holds, with any choice of $\langle O^\psi(^1S_0^{[8]}) \rangle$, there exists a set of values of $\langle O^\psi(^3S_1^{[8]}) \rangle$ and $\langle O^\psi(^3P_0^{[8]}) \rangle$ which leads to equally good description of the ψ hadroproduction and polarization data.

2) When the value of $\langle O^\psi(^1S_0^{[8]}) \rangle$ is fixed, there exists a small range of values of $\langle O^\psi(^3S_1^{[8]}) \rangle$. For any specific value of $\langle O^\psi(^3S_1^{[8]}) \rangle$ in this range, one can find a solution of $\langle O^\psi(^3P_J^{[8]}) \rangle$ leading to equally good description of the ψ hadroproduction data. However, the polarization is extremely sensitive to the choice of $\langle O^\psi(^3S_1^{[8]}) \rangle$ in this case.

3) As long as the VSR holds, the unique key parameter to govern the ψ polarization is $R_\psi \equiv \langle O^\psi(^3S_1^{[8]}) \rangle / \langle O^\psi(^3P_0^{[8]}) \rangle$. λ is extremely sensitive to R_ψ . In reverse, when R_ψ is fixed, tuning any other parameters does not affect the value of λ , but changes the ψ production results.

This brings us to a subtle circumstance where small variations of R_ψ result in equally good descriptions of the ψ production, but give totally different predictions

for the ψ polarizations. This reveals the reason why one cannot explain the ψ polarization by employing the LDMEs obtained in the fit of the yield data by minimizing χ^2 . Actually, a small deviation of the SDCs can cause slight variations of the LDMEs at which the χ^2 reaches its minimum value, but results in a big difference in the polarization results. Accordingly, the polarization is almost random if one employs the LDMEs obtained through a fit of the ψ yield data.

In this paper, we will demonstrate these features in detail, provide a procedure to fit the LDMEs, and employ them to present the polarization results.

2 Criticism of the existing fitting strategies

Before putting forward the approach, we first outline the procedures currently on the market for determining the LDMEs. Here we take the direct ψ (J/ψ , ψ') production case as an example, in which the cross section can be expressed as [1]

$$d\sigma(\psi) = \sum_n df_n \langle O^\psi(n) \rangle, \quad (2)$$

where f_n is the SDC for producing a $c\bar{c}$ pair with quantum number n , and $\langle O^\psi(n) \rangle$ is the corresponding LDME, which describes the hadronization of the $c\bar{c}$ pair and is fixed by fitting the experimental data. In the next section, we will include all the contributions to the prompt J/ψ (ψ') production.

Note that NRQCD is an effective theory, so we may expect its predictions to have an intrinsic deviation (which might not be very large, but does exist) from the reality. In addition, our concerns are always limited to specific processes (sometimes because of the lack of knowledge of other processes, which is due to e.g. experiments being lacking or higher-order corrections being large). For this reason, we regard two sets of the LDMEs leading to close predictions in the processes we are concerned with as “equivalent for these processes”. Further progress in both theoretical calculation and experimental measurement would distinguish the “equivalent” sets of LDMEs. Up to QCD NLO, ψ hadroproduction is the only process in which the dominant contributions are all counted, and at the same time, for which the corresponding experimental data are available.

When we fit the ψ yield data, the standard deviation ($\overline{\chi^2}$), which is defined as

$$\overline{\chi^2} = \frac{1}{D} \sum_d \left(\frac{\sigma_d^{th} - \sigma_d^{ex}}{\epsilon_d} \right)^2, \quad (3)$$

1) Up to the order of v^4 , the combination of $^3S_1^{[8]}$ and $^3P_J^{[8]}$ is not μ_Λ independent, unless the $^3S_1^{[1]}$ channel is included. However, for J/ψ hadroproduction, the SDC for the $^3S_1^{[1]}$ channel is very small relative to those for the other two, so we just omit this part in our discussions.

is a quadratic function of the LDMEs. Here, σ_d^{th} , σ_d^{ex} and ϵ_d denote the theoretical prediction, and the experimental central value and error for the d th experimental data point, respectively, and D is the degree of freedom in the fit. By way of illustration, we only take the three color-octet (CO) matrix elements, $\langle O^\psi(^1S_0^{[8]}) \rangle$, $\langle O^\psi(^3S_1^{[8]}) \rangle$ and $\langle O^\psi(^3P_0^{[8]}) \rangle$, as to be determined. To keep the homogeneity of the dimensions of the CO LDMEs, in this paper, we define $f_{3P_J^{[8]}}$ and $\langle O^\psi(^3P_0^{[8]}) \rangle$ by multiplying and dividing by a factor of m_c^2 , respectively. For convenience, $\langle O^\psi(n) \rangle$ is alternatively abbreviated to $\mathcal{O}_n^\psi \times 10^{-2}$ GeV³ in the following, with $n=1, 2, 3$ representing $^1S_0^{[8]}$, $^3S_1^{[8]}$ and $^3P_0^{[8]}$, respectively. Explicitly, we have

$$\begin{aligned}\mathcal{O}_1^\psi &= \langle O^\psi(^1S_0^{[8]}) \rangle / (0.01 \text{ GeV}^3), \\ \mathcal{O}_2^\psi &= \langle O^\psi(^3S_1^{[8]}) \rangle / (0.01 \text{ GeV}^3), \\ \mathcal{O}_3^\psi &= \langle O^\psi(^3P_0^{[8]}) \rangle / (0.01 \text{ GeV}^3).\end{aligned}\quad (4)$$

Note that, here, $\langle O^\psi(^3P_0^{[8]}) \rangle$ is defined by being divided by m_c^2 to keep the homogeneity of the dimension.

An ordinary fitting procedure is to solve the equations,

$$\frac{\partial \overline{\chi^2}}{\partial \mathcal{O}_n} = 0 \quad (5)$$

to fix the values of the LDMEs at which the $\overline{\chi^2}$ reaches its minimum. However, Ref. [18] found that the SDCs for the three CO channels roughly satisfy a linear relation

$$f_{3P_J^{[8]}} = r_0 f_{1S_0^{[8]}} + r_1 f_{3S_1^{[8]}}, \quad (6)$$

and thus, only two of the three LDMEs can be fixed through the fit of the yield data. For instance, the cross section for direct ψ hadroproduction can be expressed as

$$d\sigma(\psi) = f_{1S_0^{[8]}} M_0^\psi + f_{3S_1^{[8]}} M_1^\psi, \quad (7)$$

where M_0^ψ and M_1^ψ are defined by

$$\begin{aligned}M_0^\psi &= \langle O^\psi(^1S_0^{[8]}) \rangle + r_0 \langle O^\psi(^3P_0^{[8]}) \rangle, \\ M_1^\psi &= \langle O^\psi(^3S_1^{[8]}) \rangle + r_1 \langle O^\psi(^3P_0^{[8]}) \rangle.\end{aligned}\quad (8)$$

One can fit the yield data and obtain the values of M_0 and M_1 by employing Eq. (7).

The reduction strategy provided in Eq. (6) is feasible to work on the ψ yield. Nevertheless, we find that it is not suitable for the polarization problem. On the one hand, λ is sensitive to as many as two parameters, namely M_1 and r_1 ; even a slight variation of the two parameters can cause a dramatic change in λ . On the other hand, Eq. (6) is only an approximate relation; r_0 and r_1 are different in different kinematic regions (as listed in Table 1. For instance, for the CDF experimental condition, in the range $7 \text{ GeV} < p_t < 30 \text{ GeV}$, $r_0 = 3.9$ and

$r_1 = -0.56$, while in the range $11 \text{ GeV} < p_t < 30 \text{ GeV}$, $r_0 = 3.5$ and $r_1 = -0.53$. The difference of r_1 for the two p_t ranges is large enough to completely change the the polarization results.

Table 1. The values of r_0 and r_1 for different p_t ranges with $\sqrt{s}=1.96\text{TeV}$ and $m_c=1.5 \text{ GeV}$.

p_t range/GeV	6.25–30	7.5–30	10–30	11–30	40–100
r_0	4.0	3.83	3.74	3.54	7.48
r_1	-0.568	-0.550	-0.543	-0.533	-0.548

There is a parallel study on the determination of the LDMEs in Ref. [10], which employed world data for J/ ψ production and the corresponding SDCs at QCD NLO, and carried out a global fit. The LDMEs obtained were used to present the J/ ψ polarization results in Ref. [3], and the η_c hadroproduction results in Ref. [7], and it was found that they agree with none of the LHC or CDF data. These results prove that there is no one set of LDMEs which provides a good description of the data at QCD NLO. However, this does not disprove the universality of the LDMEs.

To better analyse their strategy, we express the all-order SDC as

$$f_{ao} = f_{nlo} + f_{ho}, \quad (9)$$

where f_{nlo} denotes the SDC up to QCD NLO, while f_{ho} represents the sum of the contributions of order in α_s higher than NLO. For different processes (e.g. J/ ψ hadroproduction and J/ ψ inclusive production in e^+e^- annihilation), the ratios

$$K_2(n, p_\psi) = f_{ao}(n, p_\psi) / f_{nlo}(n, p_\psi) \quad (10)$$

are expected to be different, where n is the intermediate state and p_ψ is the momentum of the ψ meson, because the significances of the higher-order corrections for different channels and in different kinematic regions are different. We cannot conclude the violation of NRQCD factorization from the nonuniversality of the LDMEs at QCD NLO.

To this end, we only focus on the J/ ψ yield and polarization data at hadron colliders, and check whether there exists a set of LDMEs which can describe all the existing data at QCD NLO, at which the SDCs for the $^3S_1^{[8]}$ and $^3P_J^{[8]}$ channels are dominated by the p_t^{-4} behavior, which is also recognized as the leading-power (LP) contributions, while that for the $^1S_0^{[8]}$ channel is dominated by the p_t^{-6} behavior, or equivalently the next-to-leading-power (NLP) contributions. Higher-order corrections cannot exceed these behaviors¹⁾, so we can expect that the QCD all-order results are proportional to the

1) At QCD NLO, the $^1S_0^{[8]}$ SDC contains the LP terms, which are very small comparing with the NLP ones. Reference [19] indicates that higher order corrections might enhance the LP contributions. However, as will be noted later, the $^1S_0^{[8]}$ channel is almost negligible. Therefore, the higher order corrections do not affect our discussions.

up-to-NLO results in medium p_t regions. This proportionality coefficient is almost constant if the rapidities are not too large. For this reason, we focus on the data in the midrapidity regions and find out whether the ψ polarization can be understood within the NRQCD framework at QCD NLO.

3 Phenomenological study of the ψ yield and polarization

In order to avoid possible large logarithm terms, our discussions are restricted to the rapidity region $|y| < 1.6$, and p_t regions $7 \text{ GeV} < p_t < 30 \text{ GeV}$ for the J/ψ and $11 \text{ GeV} < p_t < 30 \text{ GeV}$ for the ψ' [20]. The c -quark mass is set to be $m_c = 1.5 \text{ GeV}$ in the calculation of the SDCs for J/ψ , ψ' , and χ_c production. The m_c dependence of the SDCs can be balanced out by that of the LDMEs [21]. We use CTEQ6M [22] as the parton distribution function. The color-singlet LDME for the J/ψ production is taken from our previous paper [9]. Since this part is too small to affect the final results, we just use its central value, say $\langle O^{J/\psi}(^3S_1^{[1]}) \rangle = 0.645 \text{ GeV}^3$. We set $\langle O^{\psi'}(^3S_1^{[1]}) \rangle = 0.758 \text{ GeV}^3$, which is taken from Ref. [23]. The χ_c production LDMEs are taken from Ref. [17]. Their values are presented below as

$$\begin{aligned} \langle O^{\chi_{c0}}(^3P_0^{[1]}) \rangle / m_c^2 &= 0.242 \text{ GeV}^3, \\ \langle O^{\chi_{c0}}(^3S_1^{[8]}) \rangle &= (2.01 \pm 0.04) \times 10^{-3} \text{ GeV}^3. \end{aligned} \quad (11)$$

The masses [24] of the J/ψ , ψ' and χ_{cJ} ($J = 0, 1, 2$) are taken to be 3.097 GeV , 3.686 GeV , 3.415 GeV , 3.511 GeV , and 3.556 GeV , respectively. They are used to do the p_t shift, which will be mentioned later. The related branching ratios [24] are $\mathcal{B}(\psi' \rightarrow J/\psi) = 61.0\%$, $\mathcal{B}(\chi_{c0} \rightarrow J/\psi) = 1.27\%$, $\mathcal{B}(\chi_{c1} \rightarrow J/\psi) = 33.9\%$, and $\mathcal{B}(\chi_{c2} \rightarrow J/\psi) = 19.2\%$. When evaluating the feed down contributions, the p_t shift effect is considered. For instance, the p_t of a J/ψ from a ψ' with $p_t = p_t^{\psi'}$ is

$$p_t^{J/\psi} = p_t^{\psi'} m_{J/\psi} / m_{\psi'}. \quad (12)$$

The codes for computation are those developed in Ref. [5]. To calculate the χ_c feed down contribution to the polarized J/ψ , we follow the scheme developed in Ref. [5].

Reference [9] showed evidence for the VSR, which is the most fundamental basis of NRQCD (otherwise, the infinite higher excited Fock states of $c\bar{c}$ will be involved). We constrain our discussions within the scope where this rule is not violated. Under this assumption, ψ production is dominated by the combinations of the $^3S_1^{[8]}$ and $^3P_J^{[8]}$ channels.

3.1 What determines the ψ yield?

Before discussing the parameters determining the ψ yield and polarization, we directly fit the LDMEs, where

all data lying in the kinematic regions concerned in this paper in Refs. [25–29] are employed. Another two papers [30, 31] also provide data lying within our kinematic region of concern. Since these new data are consistent with the older data, we do not use them. It is impossible to fix all three CO LDMEs with only the ψ yield data, since the three CO SDCs are correlated. For this reason, we need to fix one CO LDME and fit the other two. In this section, we assign $\langle O^\psi(^1S_0^{[8]}) \rangle$ a default value, and study the dependence of the ψ hadroproduction cross sections and polarizations on the other two CO LDMEs. In the next section, we will vary $\langle O^\psi(^1S_0^{[8]}) \rangle$ and study the corresponding effects.

We set

$$\langle O^{\psi'}(^1S_0^{[8]}) \rangle = 0, \quad (13)$$

and

$$\langle O^{J/\psi}(^1S_0^{[8]}) \rangle = 0.78 \times 10^{-2} \text{ GeV}^3, \quad (14)$$

which is the central value obtained in Ref. [9]. Minimizing the χ^2 to fit the ψ' yield data, we obtain

$$\begin{aligned} \mathcal{O}_2^{\psi'} &= 0.48 \pm 0.02, \\ \mathcal{O}_3^{\psi'} &= 0.80 \pm 0.05, \end{aligned} \quad (15)$$

with $\overline{\chi^2} \approx 0.44$, where, as defined in Section 2, $\langle O^\psi(^3S_1^{[8]}) \rangle / (0.01 \text{ GeV}^3)$ and $\langle O^\psi(^3P_0^{[8]}) \rangle / (0.01 \text{ GeV}^3)$ are abbreviated as \mathcal{O}_2^ψ and \mathcal{O}_3^ψ , respectively. Employing the ψ' LDMEs, associated with the χ_c predictions, we can extract the J/ψ direct production cross sections from the prompt production cross sections, and directly fit the data to obtain

$$\begin{aligned} \mathcal{O}_2^{J/\psi} &= 1.0 \pm 0.1, \\ \mathcal{O}_3^{J/\psi} &= 1.7 \pm 0.1, \end{aligned} \quad (16)$$

with $\overline{\chi^2} \approx 1.98$, which are consistent with our previous results [9].

We remember that small deviations from the optimized values of the LDMEs provide equally good descriptions of the yield data. For this reason, we vary \mathcal{O}_3^ψ and fit \mathcal{O}_2^ψ at each specific value of \mathcal{O}_3^ψ . The results for the ψ' and J/ψ are listed in Table 2 and Table 3, respectively. Taking the J/ψ as an example, the difference between the $\overline{\chi^2}$ for $\mathcal{O}_3^{J/\psi} = 2.0$ from that for $\mathcal{O}_3^{J/\psi} = 1.7$ is only 0.3. Regarding Eq. (3), the deviation of the two curves from each other is less than 10% of the experimental error in average. Higher order corrections, experimental errors, or even the intrinsic errors of an effective theory are comparable with that. In other words, the LDMEs listed in Table 3 are equivalent for the J/ψ yield.

We can summarize the LDMEs in Table 2 and Table 3 in a compact form as

$$\mathcal{O}_2^\psi = k_\psi \mathcal{O}_3^\psi + b_\psi. \quad (17)$$

For the ψ' , we have

$$k_{\psi'}=0.42, \quad b_{\psi'}=0.143\pm 0.003, \quad (18)$$

while for the J/ψ , we have

$$k_{J/\psi}=0.367, \quad b_{J/\psi}=0.348\pm 0.011. \quad (19)$$

Table 2. The value of $\mathcal{O}_2^{\psi'}$ and the corresponding $R_{\psi'}$ and $\overline{\chi^2}$ at each specific value of $\mathcal{O}_3^{\psi'}$, while $\mathcal{O}_1^{\psi'}=0$ is set as default. The global error of $\mathcal{O}_2^{\psi'}$ is ± 0.003 .

$\mathcal{O}_3^{\psi'}$	0.50	0.60	0.70	0.80	0.90	1.00	1.10
$\mathcal{O}_2^{\psi'}$	0.353	0.395	0.437	0.479	0.521	0.563	0.605
$R_{\psi'}$	0.706	0.658	0.624	0.599	0.579	0.563	0.55
$\overline{\chi^2}$	1.23	0.79	0.53	0.44	0.53	0.79	1.22

Table 3. The value of $\mathcal{O}_2^{J/\psi}$ and the corresponding $R_{J/\psi}$ and $\overline{\chi^2}$ at each specific value of $\mathcal{O}_3^{J/\psi}$. The global error of $\mathcal{O}_2^{J/\psi}$ is ± 0.011 .

$\mathcal{O}_3^{J/\psi}$	1.50	1.60	1.70	1.80	1.90	2.00
$\mathcal{O}_2^{J/\psi}$	0.898	0.934	0.971	1.008	1.044	1.081
$R_{J/\psi}$	0.599	0.584	0.571	0.56	0.549	0.540
$\overline{\chi^2}$	2.16	2.03	1.98	2.00	2.10	2.27

Figure 1 illustrates the curves for the different LDMEs versus data. The results for the J/ψ and ψ' hadroproduction are presented in the upper and lower plots, respectively. In the upper plot, the bands are expanded by the curves for $1.7 < \mathcal{O}_3^{J/\psi} < 2.0$, with the corresponding $\mathcal{O}_2^{J/\psi}$ obtained through Eq. (17) and Eq. (19), while in the lower plot, the bands correspond to the range $0.6 < \mathcal{O}_3^{\psi'} < 1.0$, with the corresponding $\mathcal{O}_2^{\psi'}$ obtained through Equation (17) and Equation (18). It is quite obvious that all the curves lying in the bands provide

equally good descriptions of the ψ yield data. However, the values of \mathcal{O}_i^{ψ} ($i=2, 3$) are quite different. For instance, the largest value of $\mathcal{O}_3^{\psi'}$ is 1.67 times that of the smallest one. We will see in the next section that the polarization results for these different sets of the LDMEs are quite different.

3.2 R_{ψ} , the only key parameter governing the ψ polarization

Since prompt ψ hadroproduction is dominated by the ${}^3S_1^{[8]}$ and ${}^3P_J^{[8]}$ channels, the polarization of the combination of these two channels, which only depends on the ratio, $R_{\psi} \equiv \langle \mathcal{O}^{\psi}({}^3S_1^{[8]}) \rangle / \langle \mathcal{O}^{\psi}({}^3P_0^{[8]}) \rangle$, will determine the ψ polarization. Although this is true in any frame for presenting the polarization, in the present paper we restrict ourselves to the helicity frame, for illustration.

The ψ' polarization results for different sets of the LDMEs are presented in Fig. 2, where λ is defined in Eq. (1). The huge bands correspond to $0.6 < \mathcal{O}_3^{\psi'} < 1.0$, in association with the corresponding $\mathcal{O}_2^{\psi'}$ obtained through Eq. (17). From Table 2, we find that the values of $R_{\psi'}$ change slightly when the LDMEs vary under the constraint of Eq. 17. However, as shown in Fig. 2, they result in completely different values for the polarization. This proves that the polarization parameter is extremely sensitive to $R_{\psi'}$. In addition, we need to find out whether $R_{\psi'}$ is the only parameter on which the polarization depends. So, we vary $\mathcal{O}_2^{\psi'}$ from 0.6 to 1.0, at the same time keeping $R_{\psi'}$ unchanged¹⁾, and find that the deviation of λ from its central value is less than 0.01. Our work has demonstrated that $R_{\psi'}$ is the only key parameter governing the ψ' polarization, and the polarization parameter is extremely sensitive to $R_{\psi'}$. When $R_{\psi'}$ changes from 0.549 to 0.584, the change of λ can be as large as 0.5.

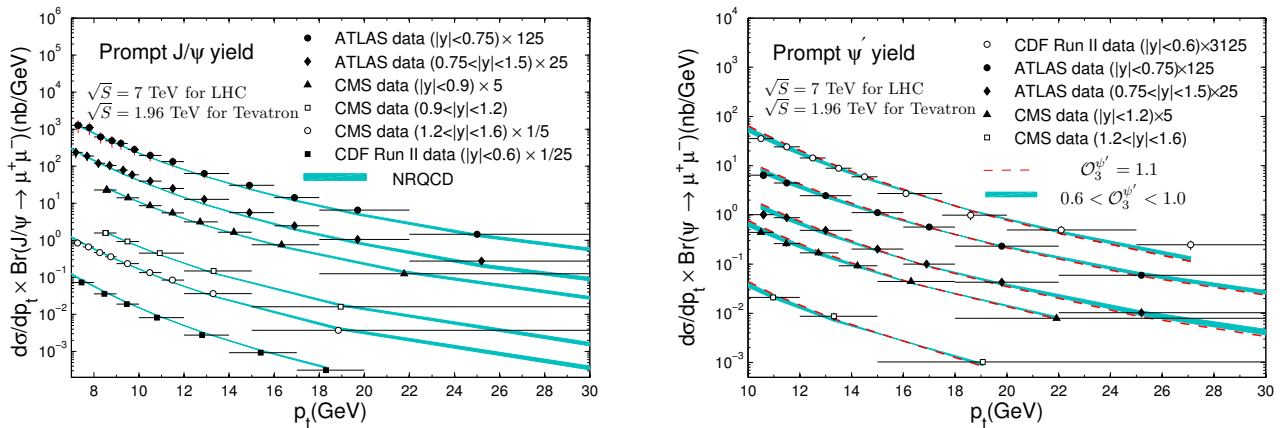


Fig. 1. (color online) J/ψ and ψ' yield at the Tevatron and the LHC in the medium p_t region. All the LDMEs follow Eq. (17) in association with Eq. (19) for J/ψ and Eq. (18) for ψ' . The data are taken from Refs. [25–29]

1) In this case, the agreement between theory and experiment on the ψ' yield will certainly be ruined.

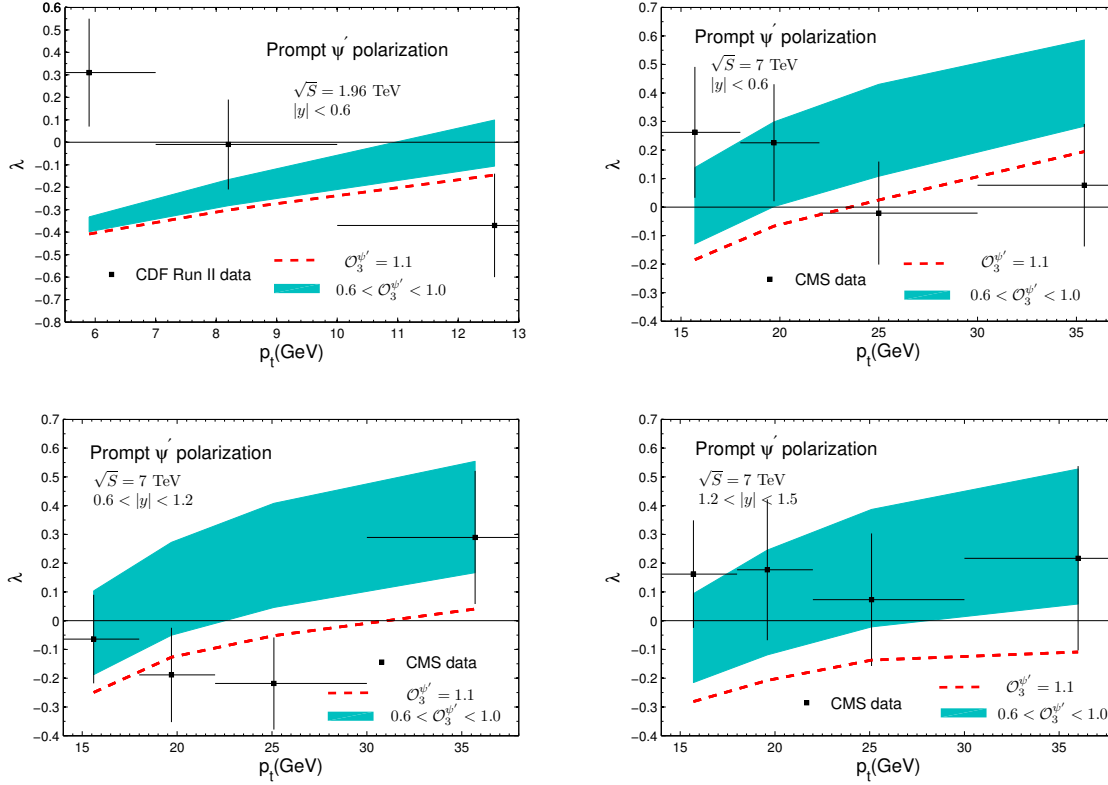


Fig. 2. (color online) ψ' polarization at the Tevatron and the LHC. All the LDMEs follow Eq. (17) and Eq. (18). The data are taken from Refs. [15, 16].

The bands in Fig. 2, although exceptionally wide, still cannot cover all the experimental data. So, we present both the ψ' yield and polarization curves (the red dashed curves) for $\mathcal{O}_2^{\psi'} = 0.605$ and $\mathcal{O}_3^{\psi'} = 1.10$. Even though the corresponding χ^2 is as large as 1.22, they can still provide good descriptions of the ψ' yield data. The errors of the ψ' polarization data are very large, and the central values of the CMS data [15] are not monotonic with respect to the transverse momentum and rapidity. We can expect precise measurements will significantly change the central values. Only when there are more precise measurements of the ψ' polarization can we make use of them to constrain the ψ' production LDMEs.

The precision of the J/ψ polarization measurement is much higher. We can therefore use these data to fix the J/ψ production LDMEs. Once $\langle O^{J/\psi}(^1S_0^{[8]}) \rangle$ is fixed and Eq. (17) and Eq. (19) are guaranteed, the degrees of freedom has been reduced to one. Since the measurements of CDF Run I and Run II contradict each other, we give up using the Run I data, because of their large uncertainties. Considering that the polarization is a ratio, even a slight error (as small as 20%) can cause significant deviation, so we drop the data in low p_t regions, where the precision provided by the perturbative expansion is quite difficult

to control. Only the $p_t > 10$ GeV data in Refs. [15, 16] are adopted in our fit. Including the contributions from χ_c and ψ' feed down, we obtain the value of $R_{J/\psi}$ as

$$R_{J/\psi} = 0.546 \pm 0.006. \quad (20)$$

We emphasize again that $R_{J/\psi}$ is the only parameter to govern the J/ψ polarization, as long as the VSR is kept. For instance, if we fix $R_{J/\psi}$ and vary $\langle O^{J/\psi}(^1S_0^{[8]}) \rangle$ from its upper to lower bound obtained in Ref. [9], or vary $\mathcal{O}_3^{J/\psi}$ from 1.5 to 2.0, the corresponding change of λ is less than 0.02 (most of the time, much smaller than this). Accordingly, Eq. (19) and Eq. (20) provide the uncorrelated form of the LDMEs; the uncertainties of $b_{J/\psi}$ and $R_{J/\psi}$ describe those of the J/ψ yield and polarization, respectively.

The solid curves in Fig. 3 are produced with the LDMEs obtained in Refs. [8, 9], which correspond to $\mathcal{O}_3^{J/\psi} = 1.7$ with Eq. (17) and Eq. (19) satisfied. The bands are produced with the LDME ranges obtained in Eq. (20), which corresponds to $1.88 < \mathcal{O}_3^{J/\psi} < 2.01$. We can see that the CMS data are described well in our framework. For the CDF data, the discrepancy between theory and experiment is larger.

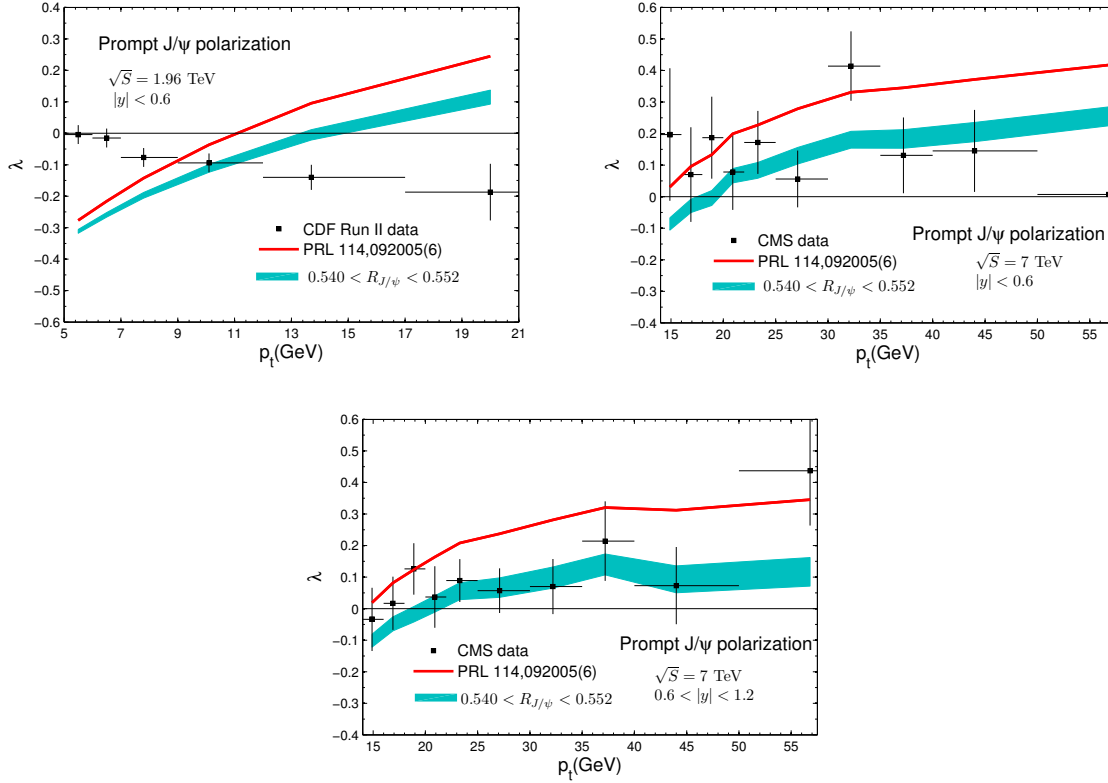


Fig. 3. (color online) J/ψ polarization at the Tevatron and the LHC. The solid curves are produced with the LDMEs obtained in Ref. [9], while the bands are produced with the LDMEs corresponding to Eq. (20). The data are taken from Refs. [15, 16].

Figures 1, 2, and 3 clearly show that when Eq. (17) is held, the yield data can be described well, while the polarization is extremely sensitive to R_ψ . This suggests it would be almost impossible to describe the polarization data using the LDMEs obtained through fitting the yield data; even when the variation of the yield curve is as slight as the intrinsic error of an effective theory, the polarization will change dramatically.

3.3 ψ yield and polarization dependence on $\langle O^\psi(^1S_0^{[8]}) \rangle$

Having got $\mathcal{O}_2^{\psi'}$ and $\mathcal{O}_3^{\psi'}$ for $\mathcal{O}_1^{\psi'} = 0$, we can attempt to assign $\mathcal{O}_1^{\psi'}$ a larger value consistent with the VSR. When $\mathcal{O}_1^{\psi'} = 1.0$, we obtain $k_{\psi'} = 0.42$ and $b_{\psi'} = 0.115 \pm 0.002$. Following the same procedure, we find that the phenomenological results do not change, which proves that varying $\mathcal{O}_1^{\psi'}$ and redoing the fitting procedure only leads to equivalent LDMEs.

We also implemented the same procedure for the J/ψ , varying $\langle O^{J/\psi}(^1S_0^{[8]}) \rangle$ from the lower to the upper bound

of the range obtained in Ref. [9]. Redoing the fit, we find that the J/ψ yield can be equally well described, and the J/ψ polarization stays unchanged once $R_{J/\psi}$ is fixed.

4 Summary

In this paper, we discovered the unique key parameter which governs the ψ polarization, namely $R_\psi \equiv \langle O^\psi(^3S_1^{[8]}) \rangle / \langle O^\psi(^3P_0^{[8]}) \rangle$. When R_ψ is fixed, the variation of the LDMEs does not change the ψ polarization if the VSR is not violated. Besides, we found that the polarization is extremely sensitive to R_ψ even under the constraint of the yield data. Accordingly, it is almost impossible to explain the polarization with the LDMEs fixed by the yield data. Having got the above features, we implemented the fit, and improved the description of CMS polarization data.

We thank Yan-Qing Ma for helpful discussions.

References

- 1 G. T. Bodwin, E. Braaten, and G. P. Lepage, *Phys. Rev. D*, **51**: 1125 (1995), [hep-ph/9407339](#)
- 2 N. Brambilla, S. Eidelman, B. Heltsley, R. Vogt, G. Bodwin, et al, *Eur. Phys. J. C*, **71**: 1534 (2011), [1010.5827](#)
- 3 M. Butenschoen and B. A. Kniehl, *Phys. Rev. Lett.*, **108**: 172002 (2012), [1201.1872](#)
- 4 K.-T. Chao, Y.-Q. Ma, H.-S. Shao, K. Wang, and Y.-J. Zhang, *Phys. Rev. Lett.*, **108**: 242004 (2012), [1201.2675](#)
- 5 B. Gong, L.-P. Wan, J.-X. Wang, and H.-F. Zhang, *Phys. Rev. Lett.*, **110**: 042002 (2013), [1205.6682](#)
- 6 R. Aaij et al (LHCb), *Eur. Phys. J. C*, **75**: 311 (2015), [1409.3612](#)
- 7 M. Butenschoen, Z.-G. He, and B. A. Kniehl, *Phys. Rev. Lett.*, **114**: 092004 (2015), [1411.5287](#)
- 8 H. Han, Y.-Q. Ma, C. Meng, H.-S. Shao, and K.-T. Chao, *Phys. Rev. Lett.*, **114**: 092005 (2015), [1411.7350](#)
- 9 H.-F. Zhang, Z. Sun, W.-L. Sang, and R. Li, *Phys. Rev. Lett.*, **114**: 092006 (2015), [1412.0508](#)
- 10 M. Butenschoen and B. A. Kniehl, *Phys. Rev. D*, **84**: 051501 (2011), [1105.0820](#)
- 11 M. Butenschoen and B. A. Kniehl, *Phys. Rev. Lett.*, **106**: 022003 (2011), [1009.5662](#)
- 12 G. T. Bodwin, H. S. Chung, U.-R. Kim, and J. Lee, *Phys. Rev. Lett.*, **113**: 022001 (2014), [1403.3612](#)
- 13 P. Faccioli, V. Knzn, C. Lourenco, J. Seixas, and H. K. 枚hri, *Phys. Lett. B*, **736**: 98 (2014), [1403.3970](#)
- 14 G. T. Bodwin, K.-T. Chao, H. S. Chung, U.-R. Kim, J. Lee, and Y.-Q. Ma, *Phys. Rev. D*, **93**: 034041 (2016), [1509.07904](#)
- 15 S. Chatrchyan et al (CMS Collaboration), *Phys. Lett. B*, **727**: 381 (2013), [1307.6070](#)
- 16 A. Abulencia et al (CDF Collaboration), *Phys. Rev. Lett.*, **99**: 132001 (2007), [0704.0638](#)
- 17 H.-F. Zhang, L. Yu, S.-X. Zhang, and L. Jia, *Phys. Rev. D*, **93**: 054033 (2016), [Addendum: *Phys. Rev. D*, **93**(7): 079901 (2016)], [1410.4032](#)
- 18 Y.-Q. Ma, K. Wang, and K.-T. Chao, *Phys. Rev. Lett.*, **106**: 042002 (2011), [1009.3655](#)
- 19 P. Artoisenet and E. Braaten, *JHEP*, **04**: 121 (2015), [1412.3834](#)
- 20 H.-S. Shao, H. Han, Y.-Q. Ma, C. Meng, Y.-J. Zhang, and K.-T. Chao, *JHEP*, **05**: 103 (2015), [1411.3300](#)
- 21 Y.-Q. Ma, K. Wang, and K.-T. Chao, *Phys. Rev. D*, **84**: 114001 (2011), [1012.1030](#)
- 22 J. Pumplin, D. R. Stump, J. Huston, H. L. Lai, P. M. Nadolsky, and W. K. Tung, *JHEP*, **07**: 012 (2002), [hep-ph/0201195](#)
- 23 E. J. Eichten and C. Quigg, *Phys. Rev. D*, **52**: 1726 (1995), [hep-ph/9503356](#)
- 24 C. Patrignani et al. (Particle Data Group), *Chin. Phys. C*, **40**: 100001 (2016)
- 25 D. Acosta et al (CDF Collaboration), *Phys. Rev. D*, **71**: 032001 (2005), [hep-ex/0412071](#)
- 26 T. Aaltonen et al (CDF Collaboration), *Phys. Rev. D*, **80**: 031103 (2009), [0905.1982](#)
- 27 G. Aad et al (ATLAS), *Nucl. Phys. B*, **850**: 387 (2011), [1104.3038](#)
- 28 S. Chatrchyan et al (CMS), *JHEP*, **1202**: 011 (2012), [1111.1557](#)
- 29 G. Aad et al (ATLAS), *JHEP*, **1409**: 79 (2014), [1407.5532](#)
- 30 G. Aad et al (ATLAS), *Eur. Phys. J. C*, **76**: 283 (2016), [1512.03657](#)
- 31 V. Khachatryan et al (CMS), *Phys. Rev. Lett.*, **114**: 191802 (2015), [1502.04155](#)